Electronic Supplementary Material (ESI) for Journal of Materials Chemistry A.

SUPPORTING INFORMATION

Bifunctional separator as a polysulfide mediator for highly stable Li-S batteries

Syed Ali Abbas[a,b,c], Mohammad Aziz Ibrahem[g], Lung-Hao Hu[d], Chia-Nan Lin[e], Jason Fang[e], KarunaKara Moorthy Boopathi[a,b,c], Pen-Cheng Wang[a], Lain-Jong Li[f], Chih-Wei Chu[c, h*]

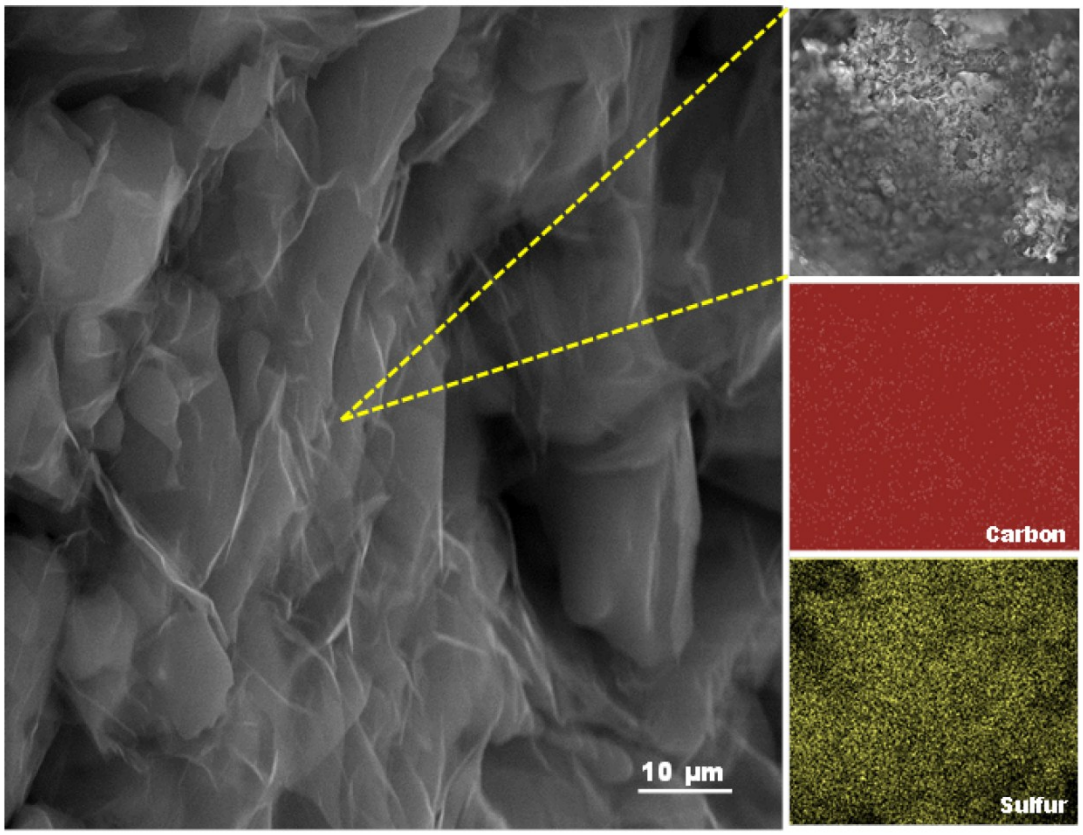

Figure S1 Scanning electron microscopy (SEM) image, with corresponding EDS maps of carbon and sulfur in the expanded graphene/sulfur electrode.

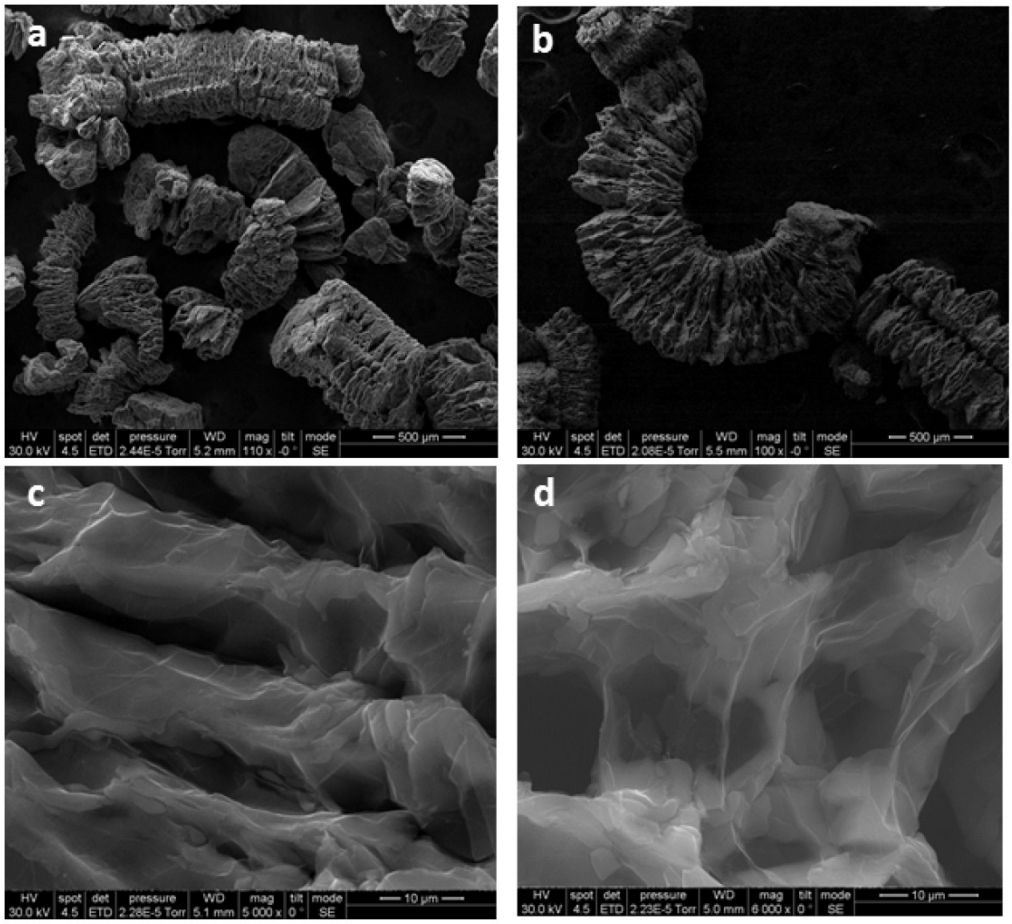

Figure S2 SEM images of an expanded graphene/sulfur at various magnifications.

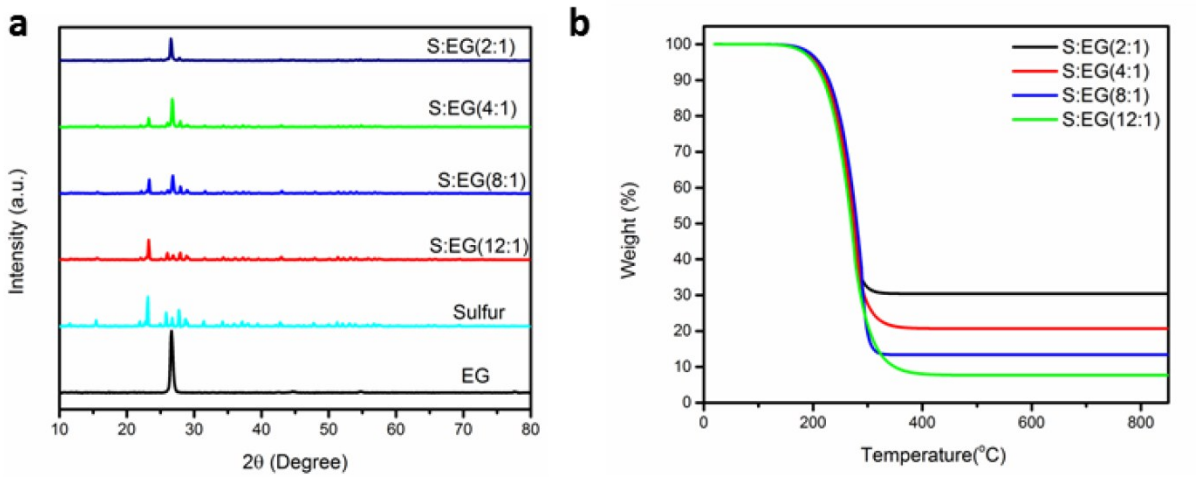

Figure S3 (a) X-ray diffraction (XRD) patterns and (b) thermogravimetric analysis (TGA) of samples prepared at various combinations of expanded graphene and sulfur.

X-ray Diffraction (XRD) Analysis

The expanded graphene/sulfur nanocomposite arrangement was clearly evident using XRD. The XRD patterns of pure expanded graphene and the expanded graphene/sulfur nanocomposites containing various sulfur contents are displayed in Figure. S3a. The XRD profile of the expanded graphene exhibited a broad, weak (002) diffraction peak at 26°, assigned to disordered stacks of graphene nanosheets. In comparison with the pattern of the expanded graphene/sulfur, the XRD patterns of the nanocomposites yielded fewer peaks of smaller intensity, indicating that sulfur was anchored mainly onto the graphene framework, with the excess sulfur forming nanosized crystalline sulfur during the cooling process. The amount of nanosized crystalline sulfur increased upon increasing the sulfur loading. As displayed in Figure S3a, when the graphene/sulfur loading ratio was 1:2, only one broad diffraction peak was evident, near 26°. It was difficult to detect any diffraction peaks for sulfur, indicating that all of the sulfur atoms existed in the graphene framework, with no excess crystalline sulfur. When the graphene/sulfur

ratio increased to 1:4, small diffraction peaks appeared in the XRD patterns of the nanocomposites, indicating the presence of the crystallized sulfur. Further loading of sulfur to levels as high as 1:8 and 1:12 resulted in sharp diffraction peaks appearing for crystallized sulfur.

Thermogravimetric Analysis (TGA)

TGA was performed under an Ar atmosphere to estimate the sulfur content in the S-G samples. Figure S3b reveals significant weight loss in the temperature range 200–400 °C for all samples, due to evaporation of impregnated sulfur. The amounts of sulfur measured in the S-G samples were 91% (1:12), 87% (1:8), 79% (1:4), and 67% (1:2), all very close to added proportions.

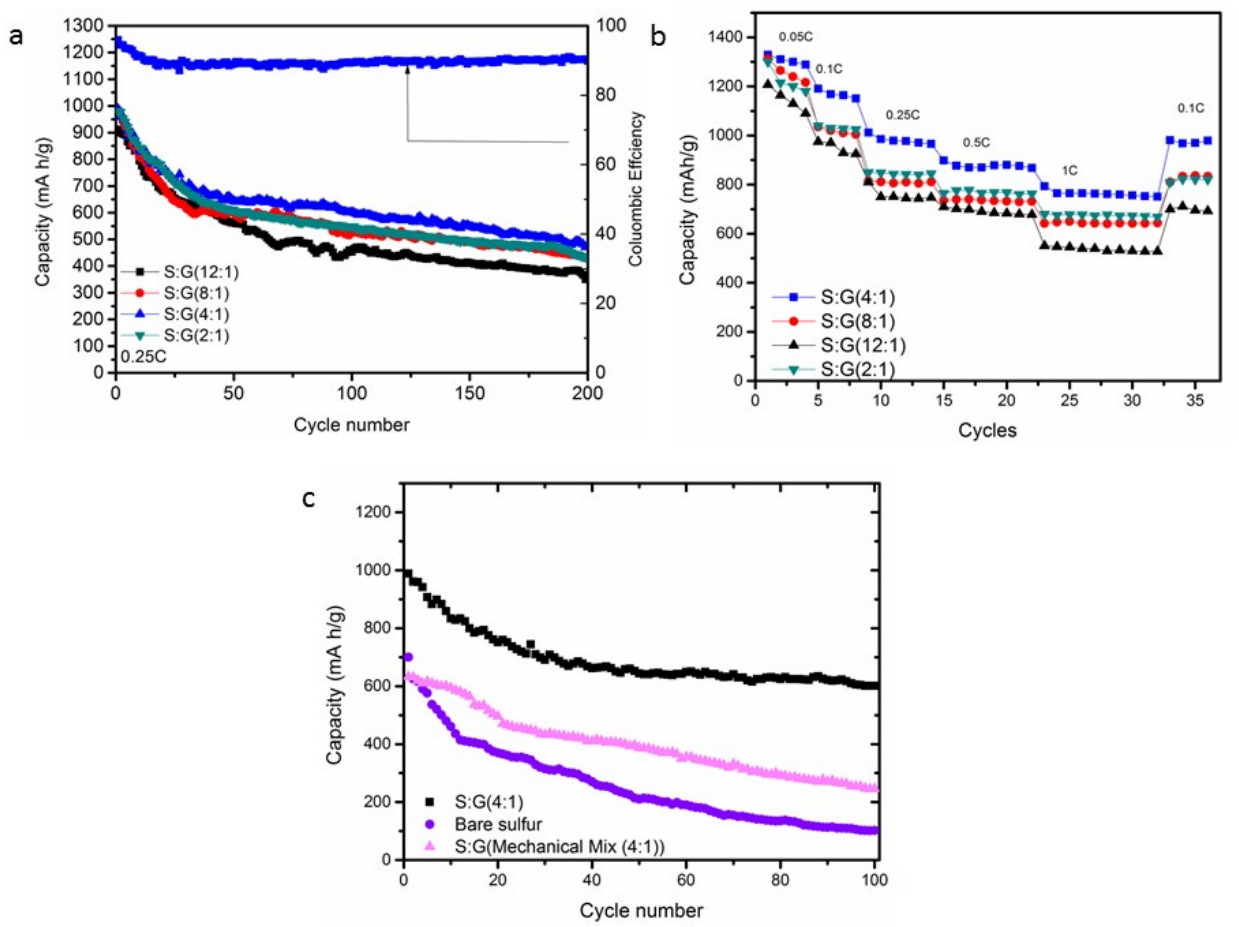

Figure S4 (a) Cycling performance of S-G samples at 0.25 C. (b) Rate capabilities of S-G samples. (c) Cycling performance of bare sulfur, S-G (4:1) after mechanical mixing with bare sulfur sulfur-infused expanded graphene S-G (4:1).

Electrochemical Cycling Performance of S:G Cathode

The electrochemical behavior of the sulfur-impregnated expanded graphene was studied through galvanostatic charge/discharge measurement. The cyclic performance of S-G samples prepared with various sulfur contents was measured at a rate of 0.25 C (1 C = 1675 mA h g^{-1}) for 200 cycles (Figure S4a). The initial discharge capacities for S-G(12:1), S-G(8:1), S-G(4:1), and S-G(2:1) were 912, 985, 988, and 981 mA h g^{-1}, respectively; after 200 cycles the capacities dropped to 359, 428, 471, and 423 mA h g^{-1}, respectively, with initial capacity retention of 39.3, 43.4, 47.6, and 43.11%, respectively. C-rate tests were performed to further evaluate the

performance of the S-G samples. Samples were discharged in a current range from 0.05 to 1 C and then reverted back to 0.1 C to compare the retention of the original capacity (Figure S4b). The results suggested that S-G(4:1) performed much better than the other combinations, retaining 82% of its original capacity [S-G(12:1), S-G(8:1), and S-G(2:1) had capacity retentions of 71.7, 78, and 77%, respectively]. For sufficient statistical significance, at least four batteries for the same sample were measured under identical conditions, with the results averaged. As a control, expanded graphene was mixed mechanically with sulfur at the same ratio as S-G(4:1) and its performance compared with that of the sulfur-impregnated expanded graphene S-G(4:1); the cycling data is presented in Figure S4c. Because the sulfur was distributed non-homogenously, the initial capacity was lower and it faded quickly.

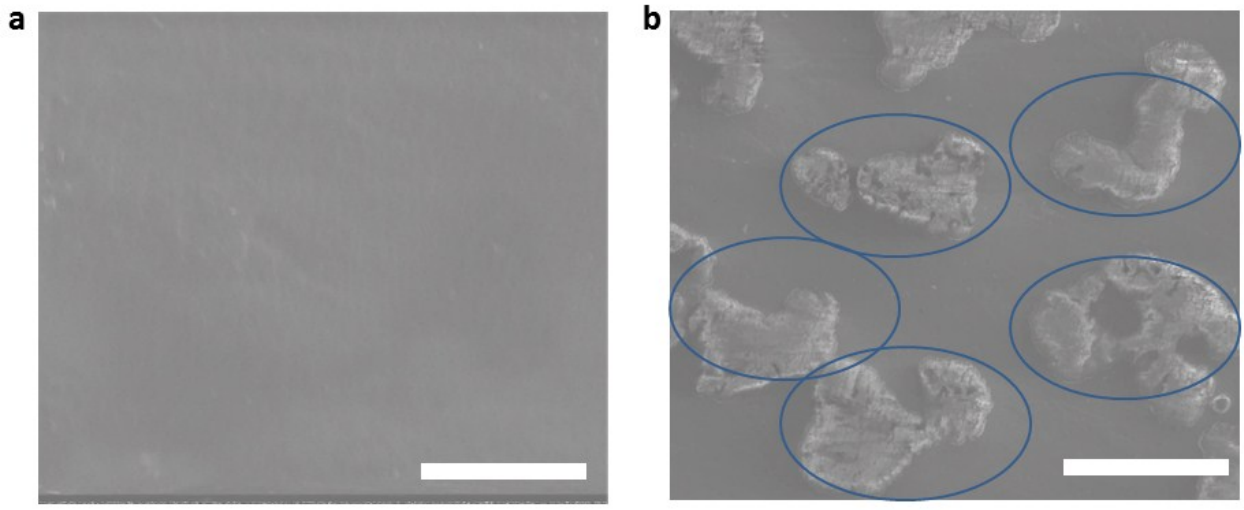

Figure. S5 SEM images of a separator featuring PEDOT:PSS loaded at (a) 0.07 mg cm^{-2} (b) 0.025 mg cm^{-2}; scale bar: 10 μm.

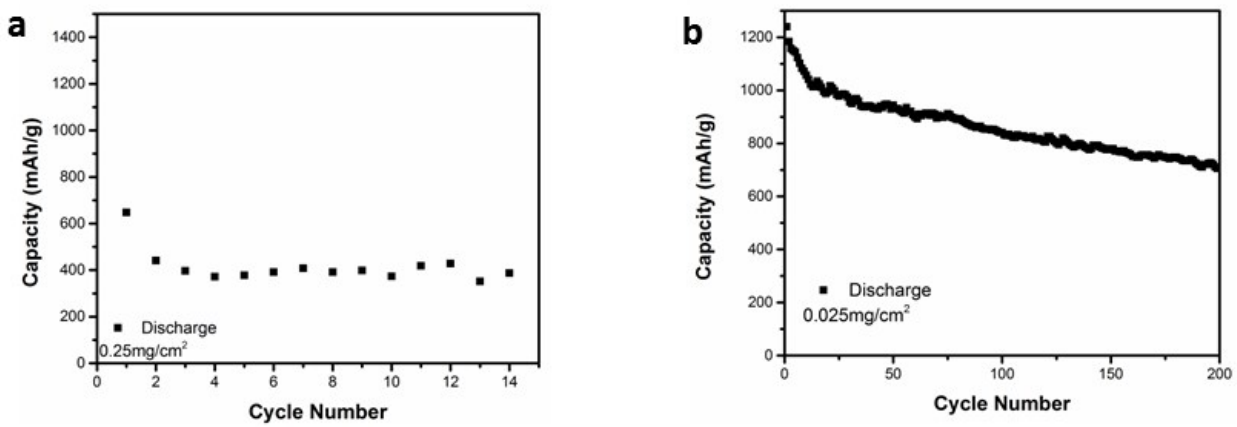

Figure. S6 Cycling performance of a separator with a PEDOT:PSS loading of (a) 0.25 mg cm^{-2} (b) 0.025 mg cm^{-2} ; at 0.25C

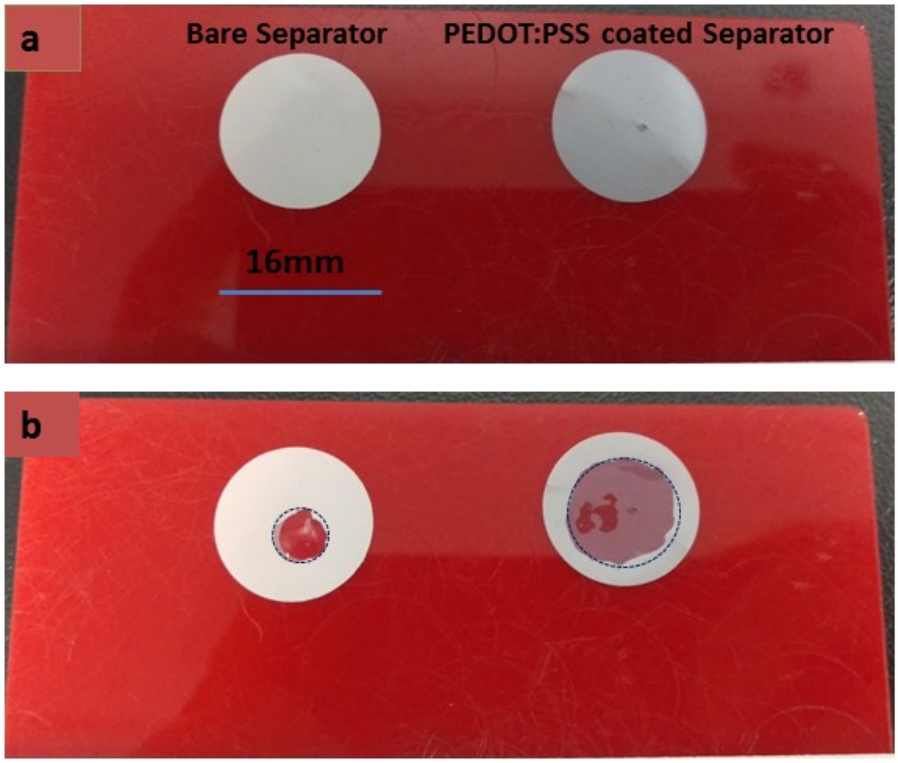

Figure S7 (a) Photographic image of bare separator on the (left) and PEDOT:PSS coated separator on the (right); (b) a simple wetting test to verify the hydrophilic character of PEDOT:PSS coated separator.

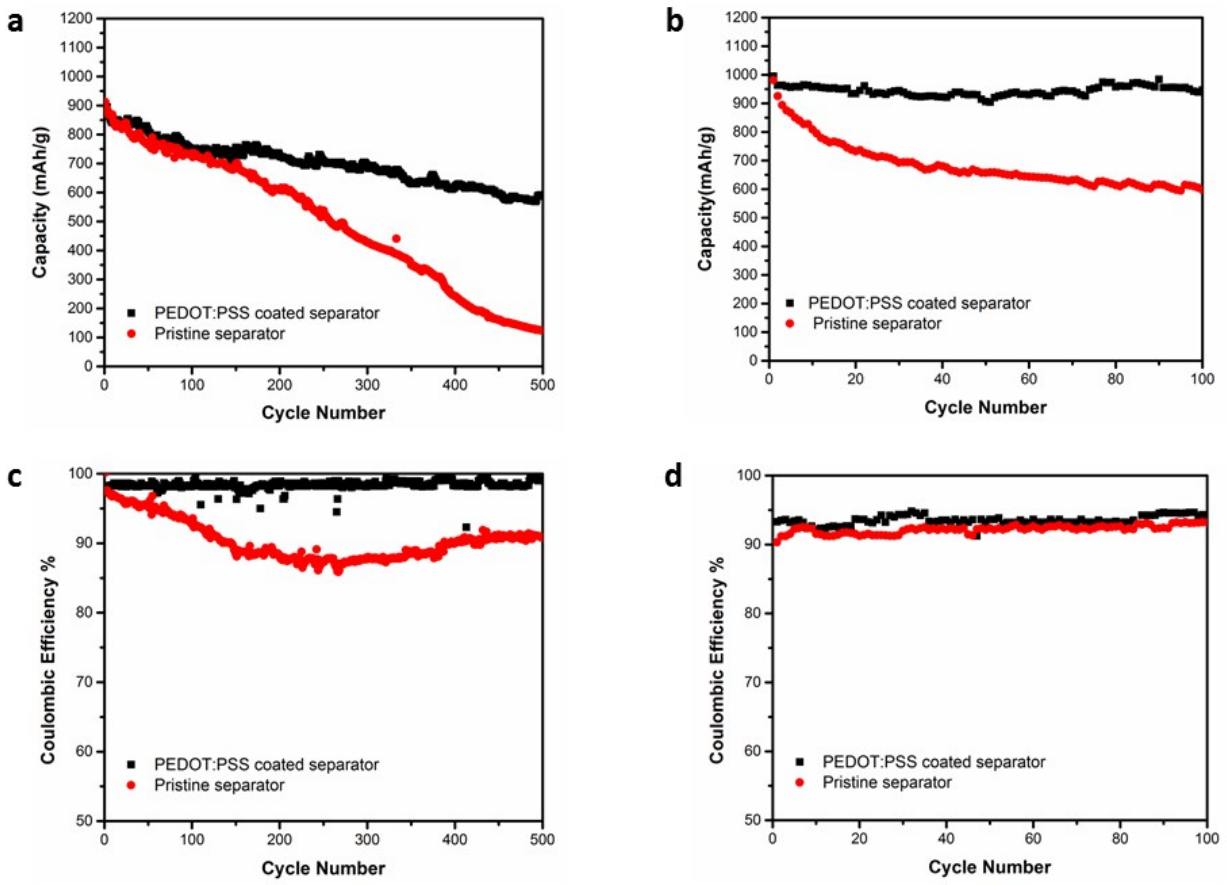

Figure S8 (a, b) Cycling data of bifunctional and pristine membranes at 0.5 and 0.1 C. (c, d) Respective coulombic efficiencies.

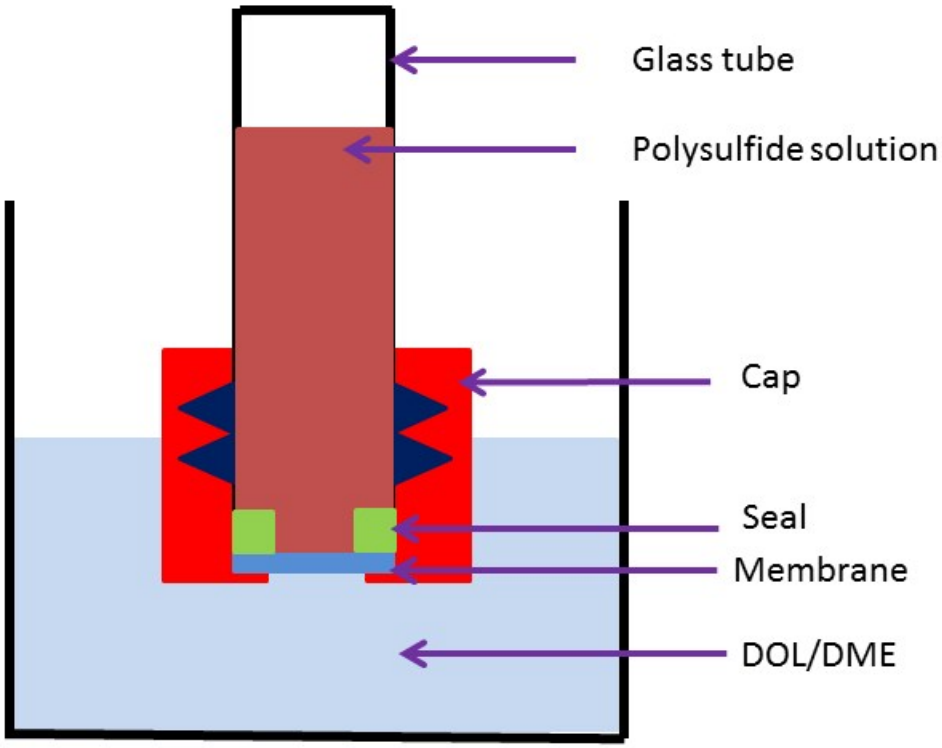

Figure S9 Schematic representation of the setup used for the polysulfide permeation tests.

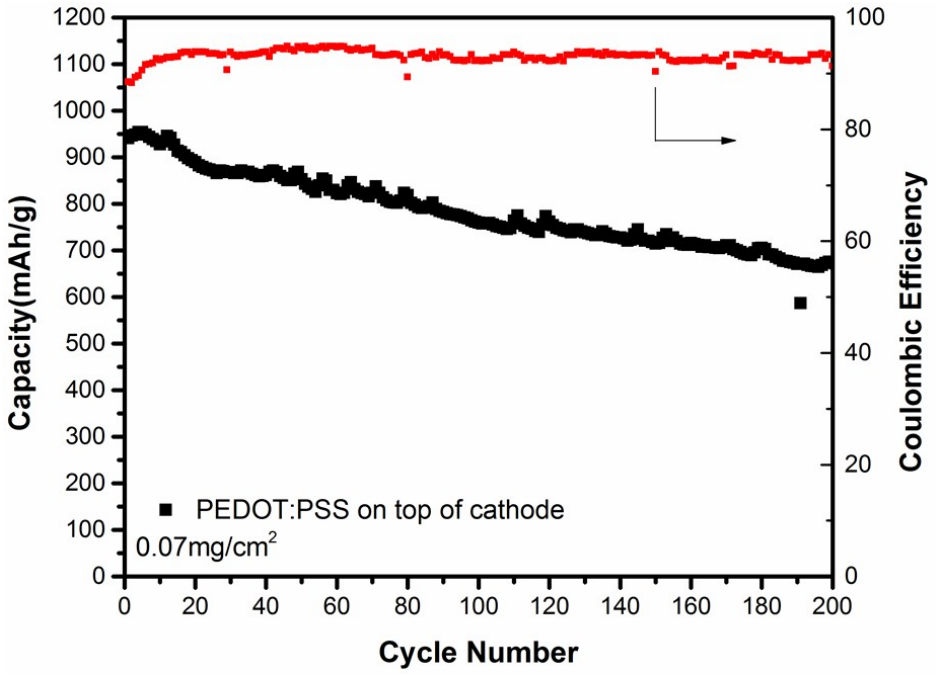

Figure S10 Cycling data of PEDOT:PSS coated at top of separator at 0.25C and respective coulombic efficiency.

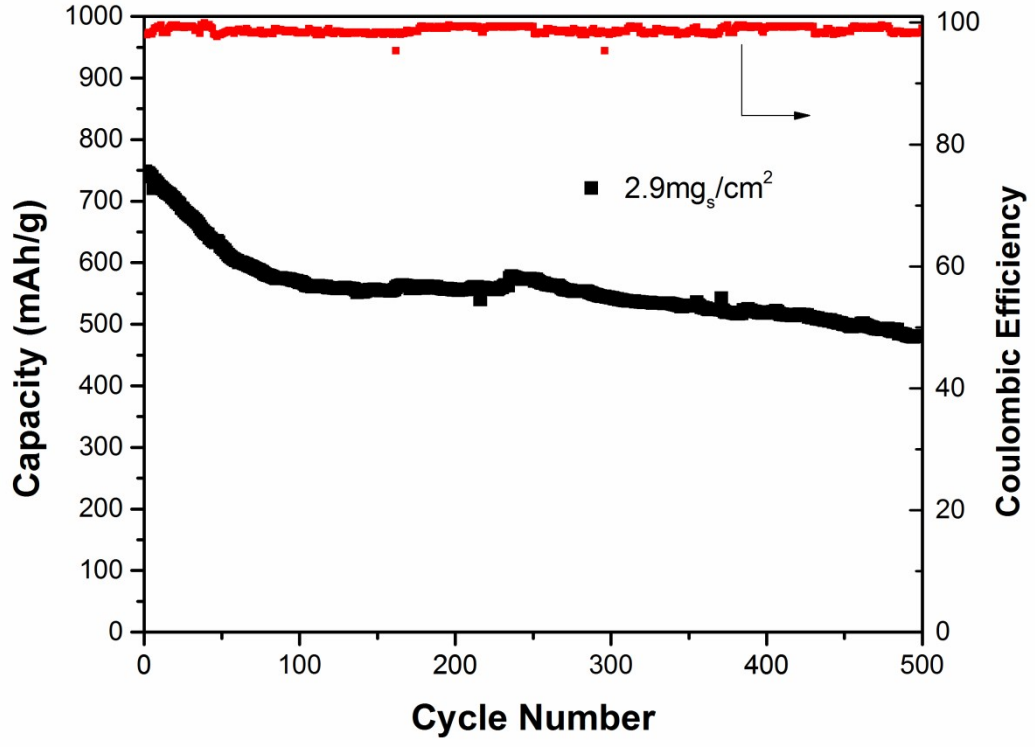

Figure S11 Cycling data of bifunctional separator at 1C with high sulfur loading of 2.9mg_s/cm^2

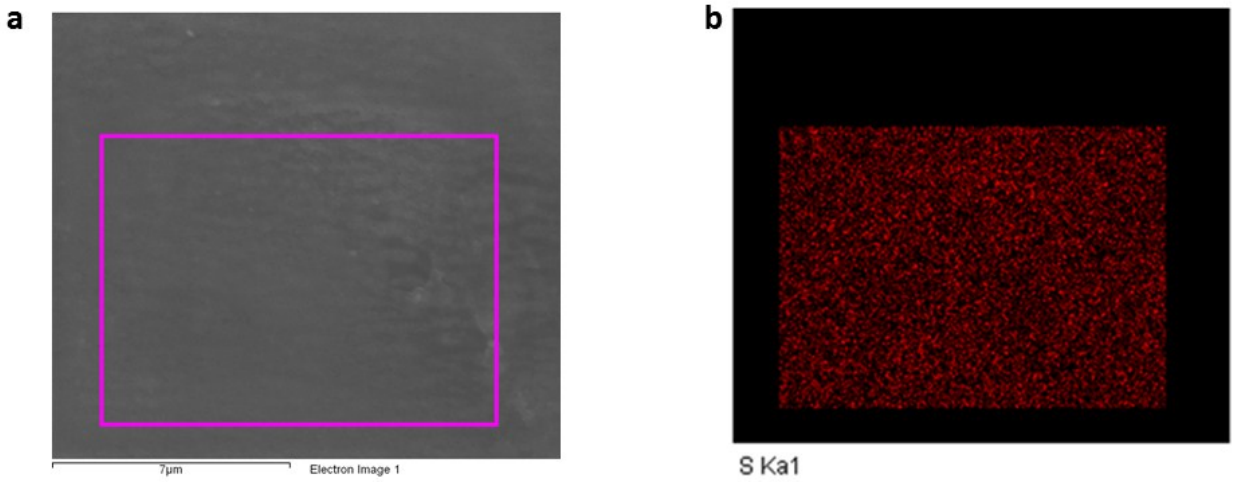

Figure S12 (a) SEM image of PEDOT:PSS coated separator after 300 cycles (b) Corresponding EDX image showing uniform distribution of sulfur on PEDOT:PSS film.